Progress In Electromagnetics Research B, Vol. 52, 307–326, 2013

ANALYSIS OF RADIAL MAGNETIZED PERMANENT MAGNET BEARING CHARACTERISTICS FOR FIVE DEGREES OF FREEDOM

Siddappa I. Bekinal[1, *], Tumkur R. Anil[1], and Soumendu Jana[2]

[1]Department of Mechanical Engineering, Gogte Institute of Technology, Belgaum 590008, Karnataka, India

[2]Propulsion Division, National Aerospace Laboratories, Bangalore 560017, Karnataka, India

Abstract—This paper presents a simple mathematical model to determine the force, stiffness and moment parameters in Permanent Magnet (PM) bearings made of radial magnetized ring magnets using Coulombian model and vector approach for five degrees of freedom. MATLAB codes are written to evaluate the bearing characteristics for three translational (x, y and z) and two angular (ξ and γ) degrees of freedom of the rotor magnet. The results of the mathematical model are compared with the results of Finite Element Analysis (FEA) using ANSYS and experiments for a PM bearing with one ring pair, thereby the presented mathematical model is validated. Furthermore, the PM bearing with three ring pairs with alternate radial polarizations is analysed by extending the presented mathematical model and also using ANSYS. Finally, the 5×5 stiffness matrix consisting of principal and cross coupled values is presented for the elementary structure as well as for the stacked structure with three ring pairs.

1. INTRODUCTION

This paper discusses the work which is the extension of the work presented in [1] by Bekinal et al., wherein the performance of the radial magnetized PM bearings was evaluated for three translational degrees of freedom of the rotor magnet. PM bearings are contact free bearings wherein the rotor is levitated by exploiting the forces generated by the magnets. These are used in many high speed applications like

Received 21 March 2013, Accepted 9 June 2013, Scheduled 17 June 2013

* Corresponding author: Siddappa Iranna Bekinal (sibekinal@git.edu).

turbo molecular pumps, energy storage flywheels, gas turbines and turbo compressors, etc. [2–4], wherein the frictionless and lubrication free operation, low maintenance and long life are the preliminary requirements. The basic analytical design relationships for magnetic field [5–9], force and stiffness [10–19] in PM bearings made of axially, radially and perpendicularly polarized ring magnets were presented by the many authors for the parametric study. In presenting the analytical equations authors have considered the following points: first, PM rings are concentric but it is not the case in actual practice (due to the presence of air gap between the stator and rotor). Secondly, most of the analytical equations are expressed in terms of elliptical integrals (first, second and third kind), Heuman's lambda function and special functions, which are tedious to deal with for five degrees of freedom of the rotor. Third, the effect of radial and angular displacements of the rotor on the force and stiffness was not considered (only one degree of freedom of the rotor was addressed). Fourth, the moment acting on the rotor due to radial and angular displacements was not addressed.

According to Earnshaw's theorem [20], the summation of bearing stiffnesses in Cartesian coordinate system must be equal to zero.

$$K_X + K_Y + K_Z = 0 \tag{1}$$

For circular rings, $K_X = K_Y = K_r$, Eq. (1) leads to

$$K_Z = -2K_r \tag{2}$$

The radial PM bearing designed to support a radial load, will be unstable in the axial direction and vice versa. To provide stability to a bearing, calculation of moment acting on the rotor magnet over a wide working range is necessary. The effect of axial, radial and angular displacements of the rotor on force and stiffness in an axially magnetized PM bearing is presented by Jiang et al. [21, 22] and Bekinal et al. [23]. This paper presents the complete analysis of the performance characteristics of the radial magnetized PM bearings by considering the axial, radial and angular displacements of the rotor using Coulombian model and vector approach. The results of the mathematical model are validated by the results of 3D FEA using ANSYS and experiments for a PM bearing with one ring pair. Finally, the stiffness matrix (Eq. (3)) representing principal and cross coupled values for five degrees of freedom is presented for an elementary structure and also for a stacked structure with three ring pairs.

$$K = \begin{bmatrix} K_{XX} & K_{XY} & K_{XZ} & K_{X\xi} & K_{X\gamma} \\ K_{YX} & K_{YY} & K_{YZ} & K_{Y\xi} & K_{Y\gamma} \\ K_{ZX} & K_{ZY} & K_{ZZ} & K_{Z\xi} & K_{Z\gamma} \\ K_{\xi X} & K_{\xi Y} & K_{\xi Z} & K_{\xi\xi} & K_{\xi\gamma} \\ K_{\gamma X} & K_{\gamma Y} & K_{\gamma Z} & K_{\gamma\xi} & K_{\gamma\gamma} \end{bmatrix} \tag{3}$$

The stiffness matrix consists of principal as well as cross coupled values in the axial, radial and angular directions. Only 15 stiffness values out of 25 have to be evaluated due to the symmetry of the matrix.

2. FORCE, STIFFNESS AND MOMENT CALCULATIONS

The basic configuration of a PM bearing with radial polarized rings and the positions of the rotor magnet with respect to translational degrees of freedom are presented in [1]. The angular movement 'ξ' of the radial magnetized rotor magnet about X-axis is shown in Fig. 1.

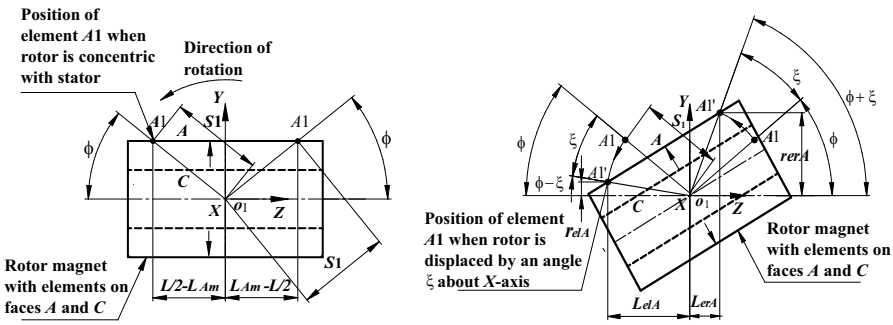

Figure 1. Positions of rotor with elements on the magnet faces. (a) Position of the rotor when it is concentric with stator. (b) Position of the rotor when it is displaced by an angle ξ about the X-axis: ϕ is the angle made by the element $A1$ with the Z-axis in YZ plane and $S1$ is the distance between the element $A1$ and the origin $O1$ in YZ plane.

The force $\vec{F}_{A1B1}$ exerted by the surface element '$B1$' on the surface element '$A1$' and the vector distance $\vec{r}_{A1B1}$ can be expressed as [1]:

$$\vec{F}_{A1B1} = \frac{\mathbf{J}^2 S_{A1} S_{B1}}{4\pi\mu_0 r_{A1B1}^3} \vec{r}_{A1B1} \tag{4}$$

$$\vec{r}_{A1B1} = (X_{B1} - X_{A1})\,\mathbf{i} + (Y_{B1} - Y_{A1})\,\mathbf{j} + (Z_{B1} - Z_{A1})\,\mathbf{k} \tag{5}$$

The positions of the elements $A1$ and $B1$ in terms of radius, mean distance from the respective centers and the angles α, β, ϕ and ξ are

expressed as (Fig. 1):

$$\begin{aligned}
&\tan(\phi) = \left(\frac{R2\sin(\beta)}{L/2 - L_{Am}}\right) \qquad S_1 = \sqrt{(R2\sin(\beta))^2 + (L/2 - L_{Am})^2} \\
&r_{elA} = S_1 \sin(\phi - \xi) \qquad r_{erA} = S_1 \sin(\phi + \xi) \\
&L_{elA} = S_1 \cos(\phi - \xi) \qquad L_{erA} = S_1 \cos(\phi + \xi) \\
&\quad \text{For } \ 0 \le L_{Am} \le L/2, \qquad \text{For } \ L/2 \le L_{Am} \le L, \\
&\qquad \vec{X}_{A1} = (x + R2\cos(\beta))\,\mathbf{i} \qquad \vec{X}_{A1} = (x + R2\cos(\beta))\,\mathbf{i} \\
&\qquad \vec{Y}_{A1} = (y + r_{elA})\,\mathbf{j} \qquad \vec{Y}_{A1} = (y + r_{erA})\,\mathbf{j} \\
&\qquad \vec{Z}_{A1} = (z + L/2 - L_{elA})\,\mathbf{k} \qquad \vec{Z}_{A1} = (z + L/2 + L_{erA})\,\mathbf{k} \\
&\quad \text{For } \ 0 \le L_{Am} \le L, \qquad \vec{X}_{B1} = (R4\cos(\alpha))\mathbf{i} \\
&\qquad\qquad\qquad\qquad\quad \vec{Y}_{B1} = (R4\sin(\alpha))\mathbf{j} \\
&\qquad\qquad\qquad\qquad\quad \vec{Z}_{B1} = L_{Bm}\mathbf{k}
\end{aligned} \tag{6}$$

where α and β are referred in XY plane (Fig. 2 of [1]), and ϕ and ξ are in YZ plane (Fig. 1). r_{elA} is the equivalent vertical distance (parallel to Y-axis) of element $A1$ from the axis of the rotor magnet, L_{Am} the mean axial distance (parallel to Z-axis) of element $A1$ from the inner magnet centre 'O',' and L_{Bm} the mean axial distance (parallel to Z-axis) of element $B1$ from the outer magnet centre 'O'.

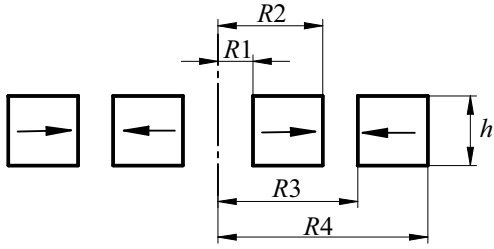

Figure 2. Cross-section view of radial magnetized PM bearing configuration with one ring pair: $R1 = 10\,\text{mm}$, $R2 = 20\,\text{mm}$, $R3 = 22\,\text{mm}$, $R4 = 32\,\text{mm}$, height of inner and outer ring $h = 10\,\text{mm}$.

Combining Eqs. (4), (5) and (6), the elemental force in terms of components in the XYZ coordinate system can be written as:

$$\vec{F}_{A1B1} = F_{A1B1X}\mathbf{i} + F_{A1B1Y}\mathbf{j} + F_{A1B1Z}\mathbf{k}. \tag{7}$$

Similarly, elemental forces $\vec{F}_{D1A1}$, $\vec{F}_{B1C1}$ and $\vec{F}_{C1D1}$ due to elements on the rotor and stator magnet surfaces A, B, C and D can

be written by considering the respective vector distances as follows (Eqs. (8)–(10)):

$$\vec{r}_{D1A1} = (X_{A1} - X_{D1})\,\mathbf{i} + (Y_{A1} - Y_{D1})\,\mathbf{j} + (Z_{A1} - Z_{D1})\,\mathbf{k} \quad (8)$$

$$\vec{r}_{B1C1} = (X_{C1} - X_{B1})\,\mathbf{i} + (Y_{C1} - Y_{B1})\,\mathbf{j} + (Z_{C1} - Z_{B1})\,\mathbf{k} \quad (9)$$

$$\vec{r}_{C1D1} = (X_{D1} - X_{C1})\,\mathbf{i} + (Y_{D1} - Y_{C1})\,\mathbf{j} + (Z_{D1} - Z_{C1})\,\mathbf{k} \quad (10)$$

where X_{C1}, Y_{C1}, Z_{C1} are the coordinate of element $C1$, and X_{D1}, Y_{D1}, Z_{D1} are the coordinate of the element $D1$. The positions of the elements $C1$ and $D1$ in terms of radius, mean distance from the respective centers and angles α, β, η and ξ can be written as:

$$\tan(\eta) = \left(\frac{R1\sin(\beta)}{L/2 - L_{Cm}}\right) \qquad S_2 = \sqrt{(R1\sin(\beta))^2 + (L/2 - L_{Cm})^2}$$

$$r_{elC} = S_2\sin(\eta - \xi) \qquad r_{erC} = S_2\sin(\eta + \xi)$$

$$L_{elC} = S_2\cos(\eta - \xi) \qquad L_{erC} = S_2\cos(\eta + \xi)$$

$$\begin{aligned}
&\text{For } 0 \le L_{Cm} \le L/2, && \text{For } L/2 \le L_{Cm} \le L,\\
&\quad \vec{X}_{C1} = (x + R1\cos(\beta))\,\mathbf{i} && \quad \vec{X}_{C1} = (x + R1\cos(\beta))\,\mathbf{i}\\
&\quad \vec{Y}_{C1} = (y + r_{elC})\,\mathbf{j} && \quad \vec{Y}_{C1} = (y + r_{erC})\,\mathbf{j}\\
&\quad \vec{Z}_{C1} = (z + L/2 - L_{elC})\,\mathbf{k} && \quad \vec{Z}_{C1} = (z + L/2 + L_{erC})\,\mathbf{k}\\
&\text{For } 0 \le L_{Cm} \le L, && \vec{X}_{D1} = (R3\cos(\alpha))\,\mathbf{i}\\
& && \vec{Y}_{D1} = (R3\sin(\alpha))\,\mathbf{j}\\
& && \vec{Z}_{D1} = L_{Dm}\mathbf{k}
\end{aligned} \quad (11)$$

where L_{Cm} is the mean axial distance (parallel to Z-axis) of element $C1$ from the inner magnet centre 'O'' and L_{Dm} the mean axial distance (parallel to Z-axis) of element $D1$ from the outer magnet centre 'O'.

Considering 'n' number of discrete elements on inner magnet surfaces and 'm' number of discrete elements on outer magnet surfaces, the resultant forces in X, Y and Z axes, are evaluated by using the equations (Eqs. (13)–(15)) presented in [1]. The bearing stiffnesses are obtained by the method of numerical differentiation after evaluating the resultant forces. The stiffness equations presented in [23] are used to determine the principal axial and radial, cross coupled radial and radial-axial stiffnesses.

The moment due to elemental force $\vec{F}_{A1B1}$ about the centre of gravity of the inner magnet can be written as:

$$\begin{aligned}
&\text{For } L/2 \le L_{Am} \le L,\\
&\quad M_{A1B1X} = -F_{A1B1Y} \times L_{erA} + F_{A1B1Z} \times r_{erA}\\
&\quad M_{A1B1Y} = F_{A1B1X} \times L_{erA} - F_{A1B1Z} \times R2\cos(\beta)\\
&\quad M_{A1B1Z} = -F_{A1B1X} \times r_{erA} + F_{A1B1Y} \times R2\cos(\beta)
\end{aligned} \quad (12)$$

For $0 \leq L_{Am} \leq L/2$,

$$\begin{aligned} M_{A1B1X} &= F_{A1B1Y} \times L_{elA} + F_{A1B1Z} \times r_{elA} \\ M_{A1B1Y} &= -F_{A1B1X} \times L_{elA} - F_{A1B1Z} \times R2\cos(\beta) \\ M_{A1B1Z} &= -F_{A1B1X} \times r_{elA} + F_{A1B1Y} \times R2\cos(\beta) \end{aligned} \tag{13}$$

Similarly, the moments due to elemental forces $\vec{F}_{D1A1}$, $\vec{F}_{B1C1}$ and $\vec{F}_{C1D1}$ about the centre of gravity of the rotor magnet can be written by following the proper sign convention. The net moments acting on the rotor magnet are evaluated by using Eqs. (28)–(30) of [1]. The equations of force, stiffness and moment due to the angular displacement of the rotor γ about the Y-axis can be derived similar to the Eqs. (4)–(13).

3. ANALYSIS OF RADIAL MAGNETIZED BEARING CONFIGURATIONS FOR FIVE DEGREES OF FREEDOM

3.1. Elementary Structure

The elementary configuration made of one ring pair (Fig. 2) is analysed for force, moment and stiffness parameters. This configuration can be used as a radial bearing as it develops positive radial force and stiffness (negative axial force and stiffness).

The axial force and stiffness parameters of the elementary configuration are calculated as a function of axial offset of the rotor magnet at different radial offset values (0.5, 0.75 and 1 mm in the positive X direction) and results are plotted in Fig. 3. Fig. 4 shows the

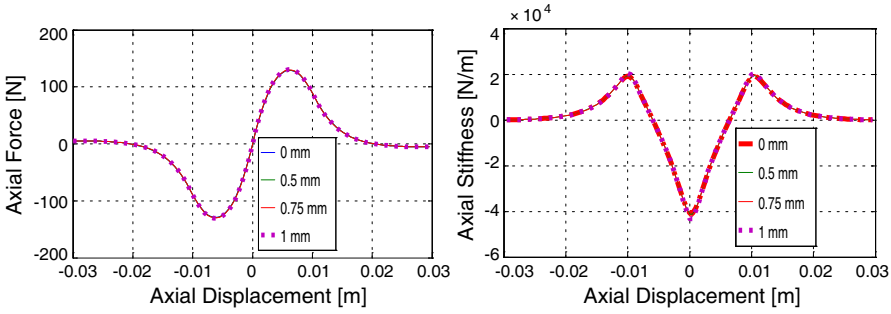

Figure 3. Characteristics of a configuration as a function of axial offset for different radial offset values of the rotor in X-axis. (a) Axial force and (b) axial stiffness.

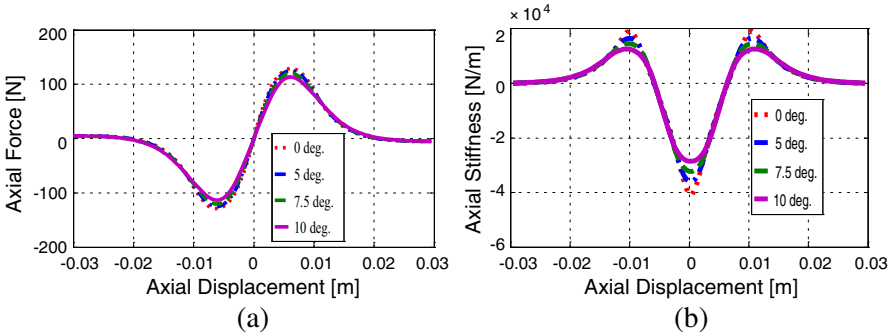

Figure 4. Characteristics of a configuration as a function of axial offset for different angular displacement values of the rotor about the X-axis. (a) Axial force and (b) axial stiffness.

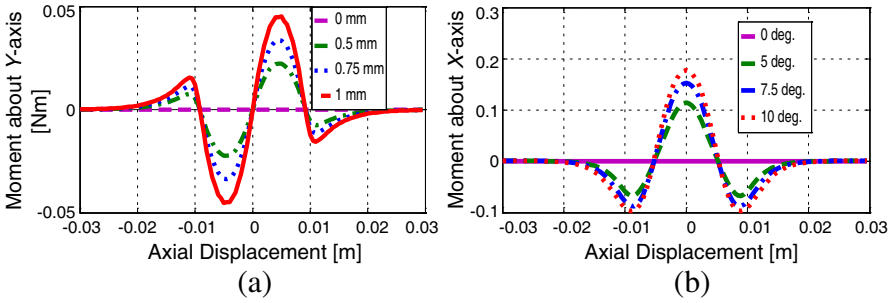

Figure 5. Moments on the rotor magnet. (a) Moment about Y-axis at various radial displacements in X-axis and (b) moment about X-axis at various angular displacements about the X-axis.

axial force and stiffness values as a function of axial offset at different angular displacement values (5°, 7.5° and 10° about the X-axis) in the configuration. The moments acting on the rotor due to its radial (0.5, 0.75 and 1 mm in the positive X direction) and angular displacements (5°, 7.5° and 10° about the X-axis) are calculated as a function of various axial positions of the rotor in the elementary configuration and results are presented in Fig. 5.

A finite element model of the elementary configuration (Fig. 2) was created in ANSYS and meshed with solid 97 elements. The maximum of number of elements considered for the analysis are 591488 (Fig. 6(a)). The properties of the magnetic material selected are: $B_r = 1\,\mathrm{T}$, $H_c = 796\,\mathrm{kA/m}$ and $\mu_r = 1.049$. The force exerted by the outer ring on the inner one is determined using a magnetic virtual

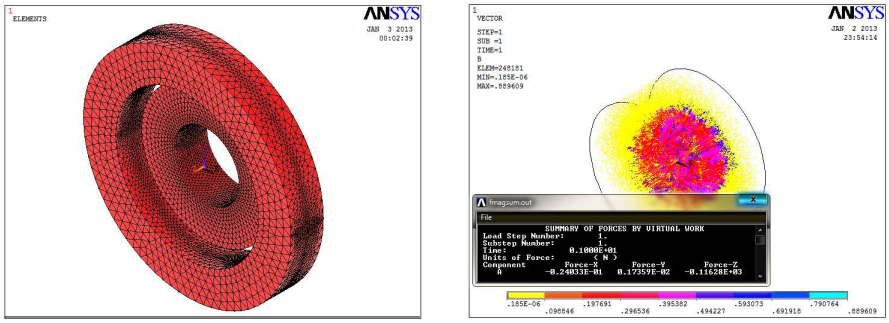

(a) (b)

Figure 6. Results of finite element analysis. (a) Arrangement of inner and outer ring magnets and (b) the maximum axial force exerted by the outer ring on the inner ring.

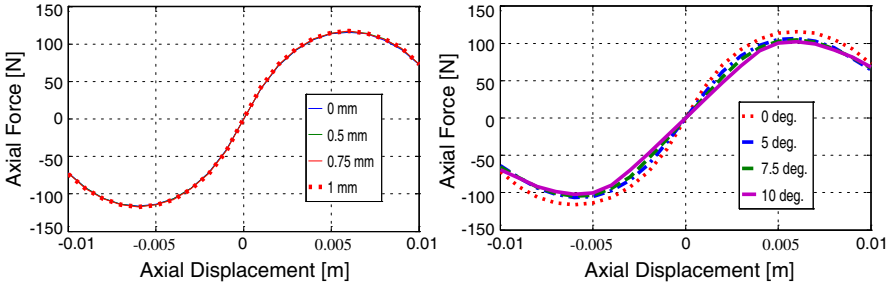

Figure 7. The axial force exerted by the outer ring on the inner ring as a function of axial offset of the rotor using finite element analysis in ANSYS. (a) Axial force at different radial displacement values and (b) axial force at different angular displacement values.

displacement approach (Fig. 6(b)). The axial force is calculated as a function of axial offset at different radial and angular displacements of the rotor magnet and results are plotted in Fig. 7.

The results shown in Figs. 3(a), 4(a) and 7 explain that the results of axial force calculated using 3D FEA using ANSYS for axial, radial and angular displacements of the rotor match closely with the results of the mathematical model. The mismatch between the results is less than 10%.

A test rig shown in Figs. 8 and 9 is designed and fabricated to measure the axial force exerted by the outer ring on the inner.

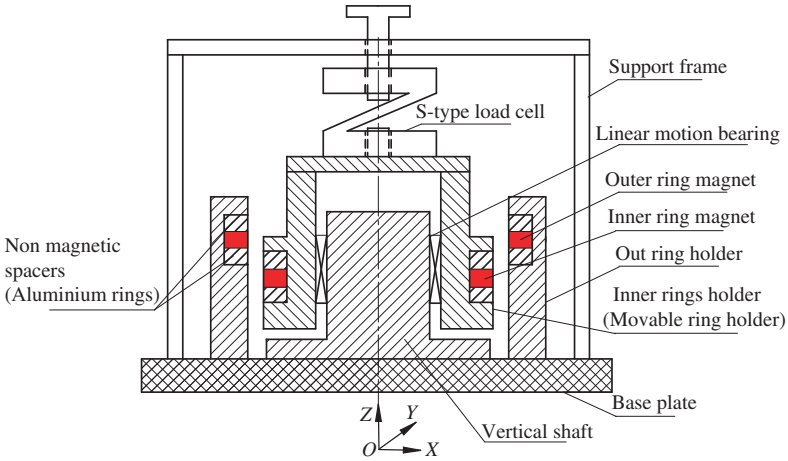

Figure 8. Schematic representation of a test rig.

Table 1. Dimensions of PM rings: inner ring composed of six sectors each of 60° and outer ring composed of eight sectors each of 45°.

Grade	$R1$ [mm]	$R2$ [mm]	$R3$ [mm]	$R4$ [mm]	h [mm]
N35 Nd-Fe-B material: $B_r = 1.2\,\mathrm{T}$, $H_c = 868\,\mathrm{kA/m}$ and $\mu_r = 1.1$.	20	25	29	34	5

The inner ring holder carries the inner ring and the outer ring is fitted to the outer ring holder with non magnetic spacers. The available magnets with the dimensions given in Table 1 are considered for the experimental work. The linear motion bearing which is provided between the inner ring holder and the vertical shaft allows the movement of the inner ring holder in the axial direction. The radial displacement of inner ring holder is achieved by displacing the vertical shaft in radial direction with a suitable base plate. The S-type load cell fitted between the inner ring holder and the support frame is used to measure the axial force at different axial displacements of the rotor. The dial gauge is used to record the axial displacements of the inner ring with respect to the outer. Suitable base plates are used to arrange the rotor concentric as well as at a radial offset of 2 mm with respect to the outer ring holder.

(a)

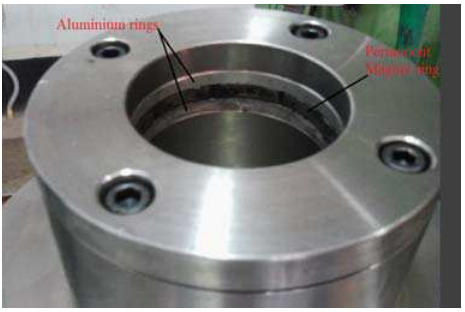

(b)

(c)

Figure 9. Details of test rig for the measurement of axial force. (a) Arrangement of rings on the inner ring holder (rotor). (b) Arrangement of rings on the outer ring holder (stator). (c) Test rig with load cell and dial gauge.

The variations of experimentally measured axial force at different axial displacements of the rotor along with the results of 3D FEA and mathematical model in the configuration at 0 mm radial displacement are shown in Fig. 10(a). The results of the experiments follow the same trend as that of mathematical model and 3D FEA. The deviation of results with respect to 3D FEA is less than 5% and with respect to mathematical model is less than 3%. The axial force is also measured at a radial offset of 2 mm and results are plotted in Fig. 10(b) along with mathematical model and 3D FEA results. The deviation of results with respect to 3D FEA is less than 4% and with respect to mathematical model is less than 3%. The discrepancy in the results might be due to non uniform magnetization of magnets.

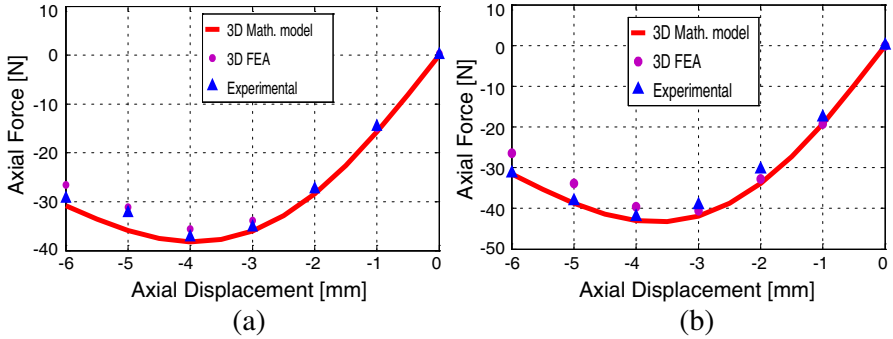

Figure 10. Results of an axial force. (a) At 0 mm radial offset. (b) At 2 mm radial offset.

Results shown in Figs. 3–5 demonstrate that the influence of radial offset on axial force and stiffness is not significant, whereas the radial displacement of the rotor in X axis generates moment about Y-axis of the rotor magnet and vice-versa. The effect of angular displacement on axial force, axial stiffness and moment is significant. Force and stiffness decrease significantly with higher values.

The angular displacement of a rotor about X-axis generates moment about the X-axis. The resultant moment about the Z axis of the rotor magnet is zero. The magnitudes of moments increase with the higher radial and angular displacement values and they vanish when the inner magnet is concentric with the outer magnet.

Figure 11 represents the radial forces and stiffness values of the

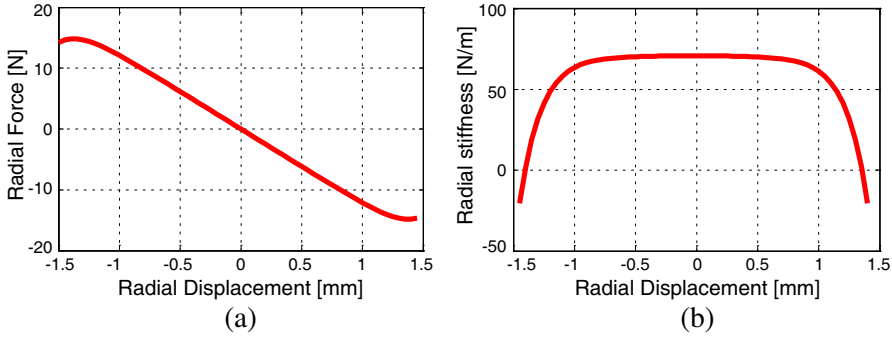

Figure 11. Characteristics of a configuration versus radial displacement in X-axis at an axial offset of 2.5 mm. (a) Radial force and (b) radial stiffness.

bearing configuration at an axial offset of 2.5 mm as a function of radial displacement. The axial force and axial stiffness of the bearing configuration calculated as a function of angular displacement about X-axis at an axial offset of 2.5 mm are shown in Fig. 12. Similarly, the moment on the rotor about the X-axis and moment stiffness at various angular displacement values are calculated at the same axial offset and results are presented in Fig. 13.

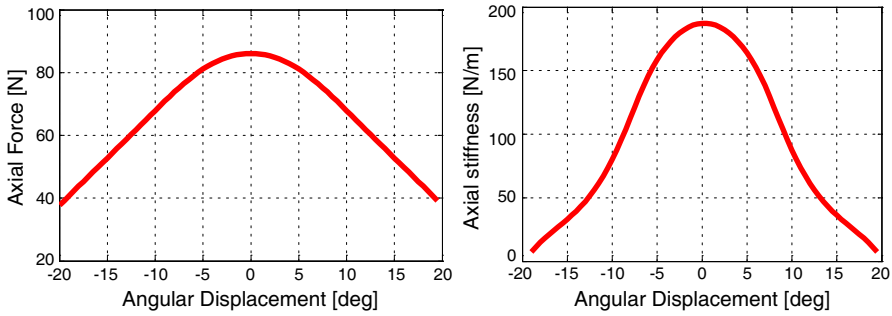

Figure 12. Characteristics of a configuration versus angular displacement about X-axis in anticlockwise direction at an axial offset of 2.5 mm. (a) Axial force and (b) axial stiffness.

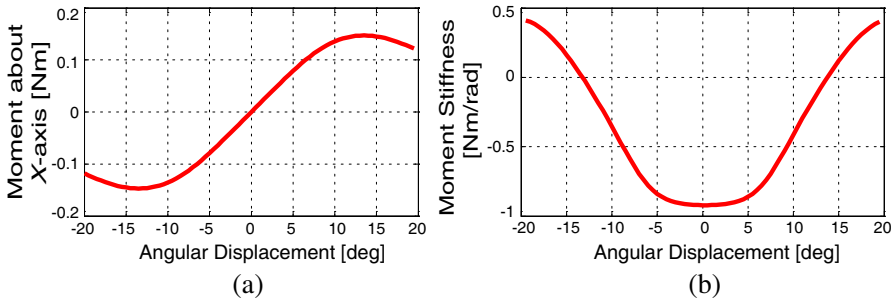

Figure 13. Characteristics of configuration versus angular displacement about X-axis in anticlockwise direction at an axial offset of 2.5 mm. (a) Moment about X-axis and (b) moment stiffness about the X-axis.

The application of a mathematical model to an elementary configuration (Fig. 2) leads to the following conclusions.

- Radial force increases with radial displacement values and radial

stiffness remains constant up to 1 mm and then decreases suddenly (Fig. 11).

- The axial force and axial stiffness decrease drastically with the angular displacement values (Fig. 12).
- Moment about X-axis increases with angular displacement and the maximum principal moment stiffness of the configuration is -0.93 Nm/rad at an angular displacement of 0° (Fig. 13).

A 5×5 stiffness matrix representing principal, cross coupled and moment stiffnesses at an axial offset of 2.5 mm in an elementary configuration is evaluated and the results are presented in Table 2. No cross coupling of stiffnesses is observed between X and Y as well as ξ and γ directions.

Table 2. Stiffness results of the configuration (Fig. 2).

	X	Y	Z	ξ	γ
X	13.54 N/mm	0	*	0	187.34 N
Y	0	13.54 N/mm	**	187.34 N	0
Z	*	**	−27.09 N/mm	#	##
ξ	0	187.34 N	#	−0.93 Nm/rad	0
γ	187.34 N	0	##	0	−0.93 Nm/rad

where $* = -12.35$ N/m at $x = 0.5$ mm $** = -12.35$ N/m at $y = 0.5$ mm
$= -25.17$ N/m at $x = 1.0$ mm $= -25.17$ N/m at $y = 1.0$ mm
$= -41.73$ N/m at $x = 1.5$ mm $= -41.73$ N/m at $y = 1.5$ mm,
and $\# = 163.94$ Nm/rad at $\xi = 5°$ $\#\# = 163.94$ Nm/rad at $\gamma = 5°$
$= 129.87$ Nm/rad at $\xi = 7.5°$ $= 129.87$ Nm/rad at $\gamma = 7.5°$
$= 87.57$ Nm/rad at $\xi = 10°$, $= 87.57$ Nm/rad at $\gamma = 10°$.

3.2. Stacked Structure with Three Ring Pairs

The stacked structure with three ring pairs with alternate radial polarizations is shown in Fig. 14. The axial force and stiffness parameters of the structure as a function of axial offset at different radial and angular displacements of the rotor are presented in Figs. 15 and 16. The moments on the rotor due to radial and angular displacements in the structure (Fig. 14) are plotted in Fig. 17.

3D FEA results of an axial force for the stacked structure at different radial and angular displacements for various axial positions of the rotor are shown in Fig. 18 and Tables 3 and 4.

The results shown in Figs. 15(a), 16(a) and 18 demonstrate that the axial force calculated using 3D FEA for axial, radial and

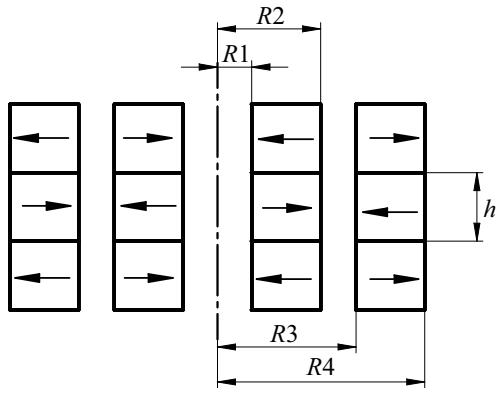

Figure 14. Cross-section view of a stacked structure composed of three ring pairs with radial polarizations: $R1 = 10\,\text{mm}$, $R2 = 20\,\text{mm}$, $R3 = 22\,\text{mm}$, $R4 = 32\,\text{mm}$, $\mathbf{J} = 1\,\text{T}$, the height of each ring permanent magnet $h = 10\,\text{mm}$.

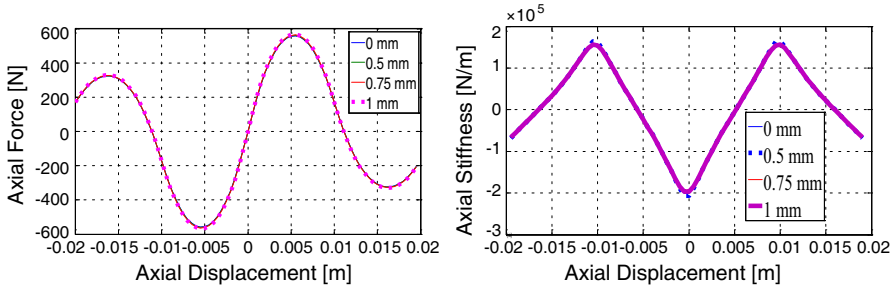

Figure 15. Characteristics of PM bearing made of three ring pairs versus axial offset at different radial displacement values in X-axis. (a) Axial force and (b) axial Stiffness.

angular displacements of the rotor match closely with the results of the mathematical model for the stacked structure. The mismatch between the results is less than 5%.

Results shown in Figs. 15–18 demonstrate that the characteristics of the stacked structure represent the same trend as that of the characteristics of the elementary configuration. The stack of three ring pairs generates higher values of axial force and axial stiffness as compared to the results of elementary configuration. The moment on the rotor increases with an increase in the number of rings in a stack. Radial forces and stiffness values calculated as a function of radial displacement of a rotor in X-axis at an axial offset of 2.5 mm

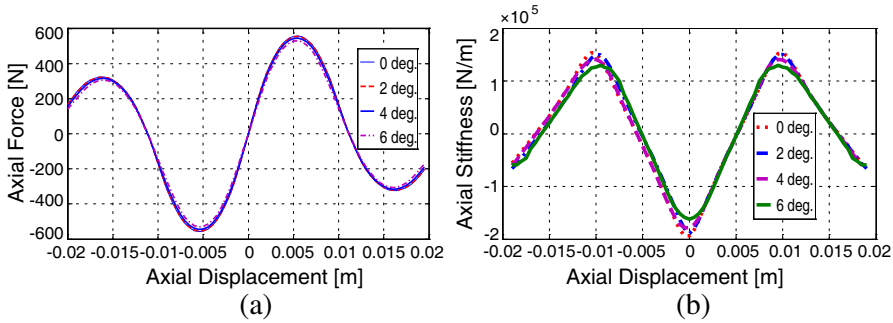

Figure 16. Characteristics of PM bearing made of three ring pairs versus axial offset at different angular displacement values about X-axis. (a) Axial force and (b) axial stiffness.

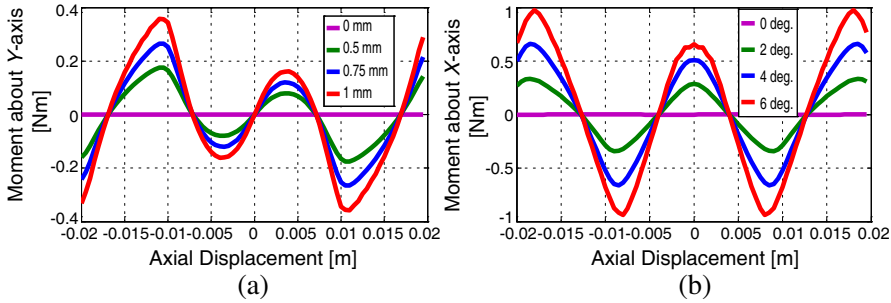

Figure 17. Moments on the rotor of a structure. (a) Moment about Y-axis due to radial displacements in X-axis and (b) moment about X-axis due to angular displacements about the X-axis.

Table 3. Results of an axial force at different radial displacements of the rotor.

Radial Displacement [mm]	0	0.5	0.75	1
Maximum Axial Force using Math. model [N]	558.64	560.71	563.53	567.54
Maximum Axial Force using ANSYS [N]	532.84	541.8	546.28	550.89

are shown in Fig. 19. Fig. 20 represents the axial force and axial stiffness variations with the angular displacement about X-axis at an axial offset of 2.5 mm. Moment on the rotor about the X-axis and

Table 4. Results of an axial force at different angular displacements of the rotor.

Angular Displacement [deg.]	0	2	4	6
Maximum Axial Force using Math. model [N]	558.64	555.36	545.98	530.2
Maximum Axial Force using ANSYS [N]	532.84	531.62	529.24	519.03

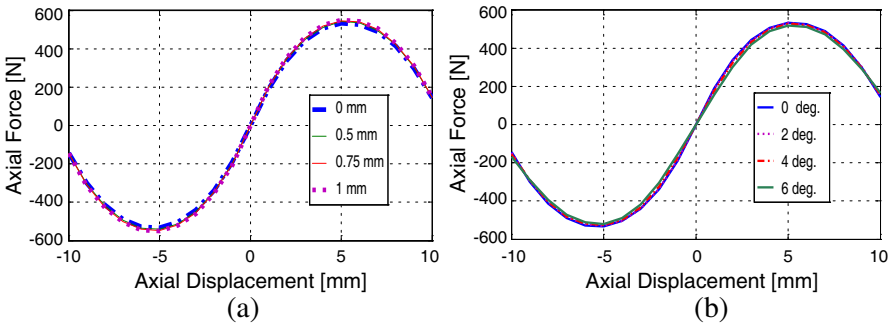

Figure 18. The axial force exerted by the stator on the rotor as a function of axial offset of the rotor using finite element analysis in ANSYS. (a) Axial force at different radial displacement values and (b) axial force at different angular displacement values.

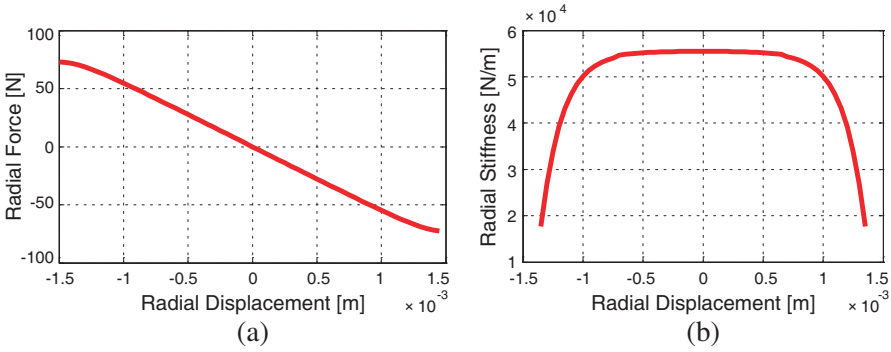

Figure 19. Characteristics of a configuration with three ring pairs versus radial displacement in X-axis. (a) Radial force and (b) radial stiffness.

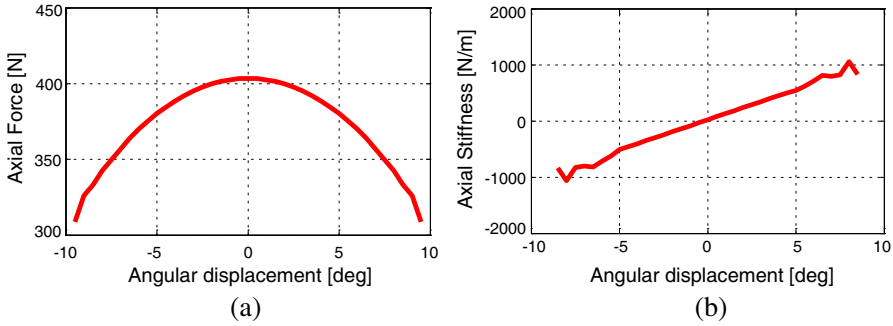

Figure 20. Characteristics of a configuration with three ring pairs versus angular displacement about the X-axis. (a) Axial force and (b) axial stiffness.

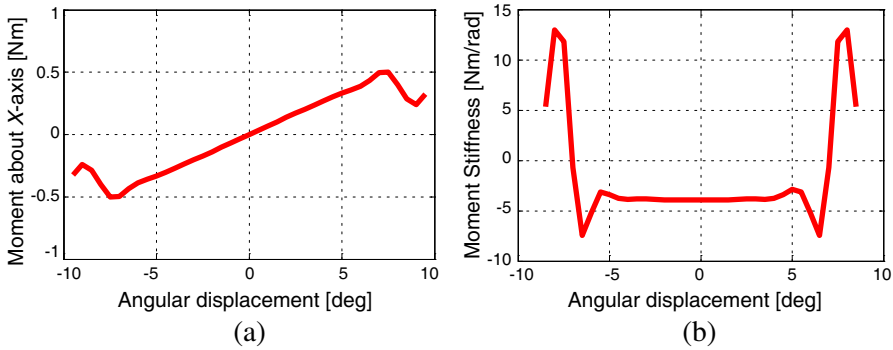

Figure 21. Characteristics of configuration with three ring pairs versus angular displacement about X-axis. (a) Moment about X-axis and (b) moment stiffness about the X-axis.

moment stiffness at various angular displacement values are calculated at the same axial offset and results are presented in Fig. 21.

The calculations of Figs. 19–21 show that the characteristics of stacked structure with three ring pairs also show the same trend as that of elementary configuration. The variation of radial stiffness of the configuration with radial displacement is almost constant up to a particular value (1 mm), then it decreases suddenly (Fig. 19(b)). The maximum principal moment stiffness of the configuration is 12.97 Nm/rad (Fig. 21(b)). A 5×5 stiffness matrix at an axial offset of 2.5 mm for the stacked structure is presented in Table 5.

Table 5. Stiffness results of the configuration (Fig. 14).

	X	Y	Z	ξ	γ
X	60.96 N/mm	0	*	0	165.1 N
Y	0	60.96 N/mm	**	165.1 N	0
Z	*	**	−121.92 N/mm	#	##
ξ	0	165.1 N	#	12.97 Nm/rad	0
γ	165.1 N	0	##	0	12.97 Nm/rad

where $* = -10.27$ N/mm at $x = 0.5$ mm $\quad ** = -10.27$ N/mm at $y = 0.5$ mm
$= -23.10$ N/mm at $x = 1.0$ mm $\quad = -23.10$ N/mm at $y = 1.0$ mm
$= -40.2$ N/mm at $x = 1.5$ mm $\quad = -40.2$ N/mm at $y = 1.5$ mm
and $\# = 240.17$ Nm/rad at $\xi = 2^\circ$ $\quad \#\# = 240.17$ Nm/rad at $\gamma = 2^\circ$
$= 455.38$ Nm/rad at $\xi = 4^\circ$ $\quad = 455.38$ Nm/rad at $\gamma = 4^\circ$
$= 711.84$ Nm/rad at $\xi = 6^\circ$ $\quad = 711.84$ Nm/rad at $\gamma = 6^\circ$.

4. CONCLUSIONS

To assist the parametric study of the optimization process, a simple mathematical model with MATLAB codes is presented to evaluate the force and stiffness parameters in PM bearings made of radial magnetized rings using Coulombian model and vector approach for five degrees of freedom of the rotor magnet. The results of the mathematical model are validated with 3D FEA and experimental results. The effects of axial and angular displacements of the rotor on the performance of the bearing are crucial: force and stiffness values are maximum at a particular value of axial offset and they decrease significantly with an increase in the angular displacement value. The effect of radial displacement is not significant and both radial and angular displacements of the rotor cause the moment on the rotor. The magnitude of the moment increases with the higher values of the displacements and also with an increase in the number of rings in the stacked structure. The presented 5×5 stiffness matrices of the configurations represent the complete performance of the radial magnetized PM bearings.

ACKNOWLEDGMENT

The authors would like to acknowledge the support of the KLS'S Gogte Institute of Technology, Belgaum and Propulsion Division, National Aerospace Laboratories, Bangalore in carrying out the research work.

REFERENCES

1. Bekinal, S. I., T. R. Anil, and S. Jana, "Analysis of radial magnetized permanent magnet bearing characteristics," *Progress In Electromagnetics Research B*, Vol. 47, 87–105, 2013.
2. Chu, H. Y., Y. Fan, and C. S. Zhang, "A novel design for the flywheel energy storage system," *Proceedings of the Eighth International Conference on Electrical Machines and Systems*, Vol. 2, 1583–1587, 2005.
3. Guilherme, G. S., R. Andrade, and A. C. Ferreira, "Magnetic bearing sets for a flywheel system," *IEEE Trans. on Applied Super Conductivity*, Vol. 17, No. 2, 2150–2153, 2007.
4. Jinji, S., R. Yuan, and F. Jiancheng, "Passive axial magnetic bearing with Halbach magnetized array in magnetically suspended control moment gyro application," *Journal of Magnetism and Magnetic Materials*, Vol. 323, No. 15, 2103–2107, 2011.
5. Ravaud, R., G. Lemarquand, and R. Lemarquand, "Analytical calculation of the magnetic field created by permanent magnet rings," *IEEE Trans. Magn.*, Vol. 44, No. 8, 1982–1989, 2008.
6. Babic, S. I. and C. Akyel, "Improvement in the analytical calculation of the magnetic field produced by permanent magnet rings," *Progress In Electromagnetics Research C*, Vol. 5, 71–82, 2008.
7. Selvaggi, J. P., et al., "Calculating the external magnetic field from permanent magnets in permanent-magnet motors — An alternative method," *IEEE Trans. Magn.*, Vol. 40, No. 5, 3278–3285, 2004.
8. Ravaud, R. and G. Lemarquand, "Comparison of the coulombian and amperian current models for calculating the magnetic field produced by radially magnetized arc shaped permanent magnets," *Progress In Electromagnetics Research*, Vol. 95, 309–327, 2009.
9. Ravaud, R., G. Lemarquand, V. Lemarquand, and C. Depollier, "Discussion about the analytical calculation of the magnetic field created by permanent magnets," *Progress In Electromagnetics Research B*, Vol. 11, 281–297, 2009.
10. Paden, B., N. Groom, and J. Antaki, "Design formulas for permanent-magnet bearings," *ASME Trans.*, Vol. 125, 734–739, 2003.
11. Chen, C., et al., "A magnetic suspension theory and its application to the heart quest ventricular assist device," *Artificial Organs*, Vol. 26, No. 11, 947–951, 2002.
12. Azukizawa, T., S. Yamamoto, and N. Matsuo, "Feasibility study

of a passive magnetic bearing using the ring shaped permanent magnets," *IEEE Trans. Magn.*, Vol. 44, No. 11, 4277–4280, 2008.

13. Lang, M., "Fast calculation method for the forces and stiffnesses of permanent-magnet bearings," *8th International Symposium on Magnetic Bearing*, 533–537, 2002.
14. Samanta, P. and H. Hirani, "Magnetic bearing configurations: Theoretical and experimental studies," *IEEE Trans. Magn.*, Vol. 44, No. 2, 292–300, 2008.
15. Ravaud, R., G. Lemarquand, and V. Lemarquand, "Force and stiffness of passive magnetic bearings using permanent magnets. Part 1: Axial magnetization," *IEEE Trans. Magn.,* Vol. 45, No. 7, 2996–3002, 2009.
16. Ravaud, R., G. Lemarquand, and V. Lemarquand, "Force and stiffness of passive magnetic bearings using permanent magnets. Part 2: Radial magnetization," *IEEE Trans. Magn.*, Vol. 45, No. 9, 3334–3342, 2009.
17. Yoo, S., et al., "Optimal design of non-contact thrust bearing using permanent magnet rings," *International Journal of Precision Engineering and Manufacturing*, Vol. 12, No. 6, 1009–1014, 2011.
18. Bekinal, S. I., T. R. Anil, and S. Jana, "Force, moment and stiffness characteristics of permanent magnet bearings," *Proceedings of National Symposium on Rotor Dynamics*, Indian Institute of Technology, 161–168, Madras, India, 2011.
19. Ravaud, R. and G. Lemarquand, "Halbach structures for permanent magnets bearings," *Progress In Electromagnetics Research M*, Vol. 14, 263–277, 2010.
20. Earnshaw, S., "On the nature of the molecular forces which regulate the constitution of the luminiferous ether," *Transactions of the Cambridge Philosophical Society*, Vol. 7, 97–112, 1842.
21. Jiang, W., et al., "Forces and moments in axially polarized radial permanent magnet bearings," *Proceedings of Eighth International Symposium on Magnetic Bearings*, 521–526, Mito, Japan, 2002.
22. Jiang, W., et al., "Stiffness analysis of axially polarized radial permanent magnet bearings," *Proceedings of Eighth International Symposium on Magnetic Bearings*, 527–532, Mito, Japan, 2002.
23. Bekinal, S. I., T. R. Anil, and S. Jana, "Analysis of axially magnetized permanent magnet bearing characteristics," *Progress In Electromagnetics Research B*, Vol. 44, 327–343, 2012.